Bond graph model of a flapping wing micro-air vehicle

Samuel Dupont, Sébastien Grondel, Alexandre Bontemps, Eric Cattan, Daniel Coutellier

Bond graph model of a flapping wing micro-air vehicle

Dupont Samuel, Grondel Sébastien, Bontemps Alexandre, Cattan Eric
Université Lille Nord de France
IEMN, UMR 8520
Université de Valenciennes
59313 Valenciennes
Samuel.dupont@univ-valenciennes.fr

Coutellier Daniel
Université Lille Nord de France
LAMIH, UMR 8530
Université de Valenciennes
59313 Valenciennes

***Abstract*. Birds and insects demonstrate impressive aerial capacities in terms of hovering, backward flight or sudden acceleration and their diversity brings multiple solutions to design micro- and nano-air vehicles (MAV's and NAV's). To allow a remotely flight control of such vehicles, many scientific and technological challenges have to be solved. First, it is necessary to mimic the flapping of an insect or bird in order to produce sufficient lift forces. Second, the conception and the design of the vehicle must integrate not only the design of the structure but also implement the electronic control functionalities.**

Within this context, this work presents a dynamic Bond Graph model of a flapping wing MAV. The objective is to use this model in order to better understand the flapping flight performed in nature. The Newton-Euler formalism with body fixed coordinates is chosen to model the dynamics of the MAV which features a body and two wings along which the aerodynamics efforts are integrated. Moreover, the graphical nature and explicit power flow path inherent in the Bond Graph facilitates model construction and troubleshooting. Open-Loop simulations are performed using commercial existing software and compared successfully with experimental data published on the RoboFly.

Keywords—Bond Graph, MAV, dynamic model, flapping wings

I. Introduction

Unmanned Aerial Vehicles (UAV's) enjoy the latest technology and seem ready to conquer the civilian and defence markets. In particular, a great interest is focused on micro-air vehicles (MAV's) and nano-air vehicles (NAV's) which expand the applications of more traditional UAV's due to their high manoeuvrability, portability and aeromechanical propulsion efficiency. The development of miniaturized structures, propulsion and navigation systems, aerodynamics, flight controllers, actuators and sensors are just a few of the current research topics in the field of MAV and NAV as shown in the last edition of the International Competition of Micro Aerial Vehicle and Flight competition (IMAV 2013) [1]. Among those topics, flapping MAVs are subject to a growing interest. They are inspired by insects and birds and fly by generating lift through oscillation or flapping of wings [2].

The first active flapping MAV reviewed was the Terrestrial Entomopter: it was constructed of the Reciprocating Chemical Muscle (RCM) actuator and stereolithographic wings. Flight control was achieved through the actuation of the x-wing design of the system. The University of Delft [3] proposed a MAV called the DelFly micro which was able to fly in outdoor and indoor for several minutes. This MAV only weighed 3 grams and had a size of 10cm from wing tip to wing tip. This makes it the smallest flying ornithopter carrying a camera in the world. From its side, Defence Advanced Research Projects Agency (DARPA) contributed to create a prototype "hummingbird-like" aircraft for a "NAV" program [4]. The result was called the Nano Hummingbird which can fly at 18km/h and move in three axes of motion. The artificial hummingbird manoeuvres using its flapping wings for propulsion and attitude control. It includes the systems required for flight: batteries, motors, and communications systems as well as the video camera payload.

By scaling down prototypes around a wingspan of 3-5 cm, NAV's are scarce [5] and only the tiny fly by Wood *et al.* [6] is currently capable of flying under tethered power supply. Novel fabrication methods, design strategies as well as actuation concepts are here mandatory and micro-electro-mechanical systems (MEMS) technologies offer a very attractive solution by providing reliable, accurate and efficient microstructures such as required by a flapping-wing NAVs. To our knowledge, IEMN is the only ones to propose an entire MEMS structure called OVMI [7-8] able to produce large displacement and lift through the use of an electromagnetic actuator.

The modelling and control of insect-like flapping wing MAV and NAV is widely studied and continuing to expand. Many of the research present in the literature focus on the standard aircraft six degrees of freedom equations found in many flight

dynamics textbooks, e.g., the treatment by Etkin and Reid [9]. For example, Doman *et al.* [10-11] present modelling and control of a flapping wing MAV based on the RoboFly presented in [12]. The aerodynamic model used in the simulations is developed in [13] and based on the work of Sane and Dickinson in [14]. The standard aircraft equations of motion are justified here by assuming that either acceleration or the gyroscopic effects of the wings are small, compared to the body effects, or that the effects averaged over one flapping cycle are identically zero. An alternative approach is to use a combination of analysis and experimentation. For example, Perez *et al* [15] propose a two-stage methodology for tackling the problem: in the first stage, substantial a priori information about the system is gathered through system identification; in the second stage, the information collected through the static flapping experiments is employed to design the controller used in vertical flight. The design of the proposed controller relies on the idea of treating an exciting signal as a subsystem of the NAV.

Since the controlled flight of our NAV [8] requires optimizing the actuation in terms of power consumption, this paper introduces Bond Graph modelling to the field of flapping UAV's. Indeed, we chose to use language software adapted to mechatronic systems and energetic study. Our long-term goal is to build a full system description model, including the power actuation-transmission system [16] and the dynamic behaviour of the OVMI. As a first step, we focus in this paper on the Bond graph dynamics modelling of a MAV similar to the RoboFly in order to validate our modelling approach.

II. Flapping Wing MAV

A. Global dynamics equations

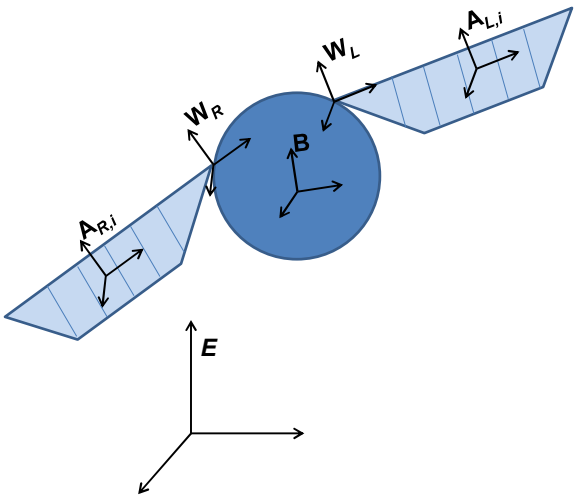

Fig. 1. Flapping wing MAV schematic with reference frames.

To derive the equation system of the flapping wing MAV, we assume that the wings are rigid and that the MAV structure is symmetric. Figure 1 shows the coordinate system for the two models. The earth frame is denoted: $\boldsymbol{E}$ (E; $\boldsymbol{x_E}$, $\boldsymbol{y_E}$, $\boldsymbol{z_E}$) and the body frame is denoted $\boldsymbol{B}$ (B; $\boldsymbol{x}$, $\boldsymbol{y}$, $\boldsymbol{z}$). The right (left) wing frame is denoted $\boldsymbol{W_R}$(W_R; $\boldsymbol{x_R}$, $\boldsymbol{y_R}$, $\boldsymbol{z_R}$) ($\boldsymbol{W_L}$(W_L; $\boldsymbol{x_L}$, $\boldsymbol{y_L}$, $\boldsymbol{z_L}$)), W_R and W_L being the articulation points of the right and left wings respectively. Another important frame is the aerodynamic frame $\boldsymbol{A_{L,i}}$ ($\boldsymbol{A_{R,i}}$), which corresponds to the right (left) aerodynamic frame of the i^{th} wing element with origin the aerodynamic centre of pressure.

Assuming that the mass and inertial of the wings as well as the aerodynamic forces on the body are negligible, the equations of motion of the flapping wing MAV developed in the Newton-Euler formalism can be expressed as:

$$\mathbf{F}_{\mathbf{ext}} = m\dot{\mathbf{V}}_{\mathbf{B}} + \boldsymbol{\Omega}_{\mathbf{EB}} \otimes m\mathbf{V}_{\mathbf{B}} \tag{1}$$

$$\mathbf{M}_{\mathbf{ext}} = I_b \dot{\boldsymbol{\Omega}}_{\mathbf{EB}} + \boldsymbol{\Omega}_{\mathbf{EB}} \otimes I_b \boldsymbol{\Omega}_{\mathbf{EB}} \tag{2}$$

with m, I_b being the body mass and inertia tensor about its respective centre of mass, whereas $\mathbf{V_B}$ and $\boldsymbol{\Omega}_{\mathbf{EB}}$ are the translational velocity with respect to the earth frame and the angular velocity of the body with respect to the earth frame expressed in the body frame respectively. Moreover, $\mathbf{F_{ext}}$ and $\mathbf{M_{ext}}$ stand for the sum of external forces and moments applied at the centre of mass, namely: gravitational and aerodynamic efforts.

$$\mathbf{F}_{\mathbf{ext}} = \mathbf{F}_{\mathbf{aero}} + m\mathbf{g} \tag{3}$$

$$\mathbf{M}_{\mathbf{ext}} = \mathbf{M}_{\mathbf{aero}} \tag{4}$$

To express the dynamic resultant $\mathbf{F_{aero}}$ and moment $\mathbf{M_{aero}}$ of the aerodynamic forces, the local aerodynamic forces and moments must be converted from the aerodynamic frame to the earth frame.

$$\begin{aligned}\mathbf{F}_{\mathbf{aero}} &= \mathbf{F}_{\mathbf{aeroR}} + \mathbf{F}_{\mathbf{aeroL}} \\ &= \mathbf{R}_{EB}\mathbf{R}_{BW_R}\sum_i \mathbf{R}_{W_R A_{R,i}} \begin{pmatrix} D_{R,i} \\ 0 \\ L_{R,i} \end{pmatrix} + \mathbf{R}_{EB}\mathbf{R}_{BW_L}\sum_i \mathbf{R}_{W_L A_{L,i}} \begin{pmatrix} D_{L,i} \\ 0 \\ L_{L,i} \end{pmatrix}\end{aligned} \tag{5}$$

where $\mathbf{F_{aeroR}}$ and $\mathbf{F_{aeroL}}$ denote the aerodynamic forces within the earth frame, whereas $D_{R,i}$, $D_{L,i}$ and $L_{R,i}$, $L_{L,i}$ represent the drag and lift components on the i^{th} chord-length element of the right and left wings respectively. Here $\mathbf{R}_{EB}$ (resp. $\mathbf{R}_{BW}$) is the rotation matrix between the earth frame and the body frame (resp. between the body frame and the wing frame) whereas $\mathbf{R}_{WAi}$ corresponds to the rotation matrix between the wing frame and the aerodynamic frame of the i^{th} wing element.

$$\begin{aligned}\mathbf{M_{aero}} &= \mathbf{M_{aeroR}} + \mathbf{M_{aeroL}} = \vec{BA}_R \otimes \mathbf{F_{aeroR}} + \vec{BA}_L \otimes \mathbf{F_{aeroL}} \\ &= \mathbf{R}_{BW_R} \sum_i \left[\mathbf{R}_{W_R B} \begin{pmatrix} x_{WR} \\ y_{WR} \\ z_{WR} \end{pmatrix} + \begin{pmatrix} x_{AR,i} \\ y_{AR,i} \\ 0 \end{pmatrix} \right] \otimes \mathbf{R}_{W_R A_{R,i}} \begin{pmatrix} D_{R,i} \\ 0 \\ L_{R,i} \end{pmatrix} \\ &+ \mathbf{R}_{BW_L} \sum_i \left[\mathbf{R}_{W_L B} \begin{pmatrix} x_{WL} \\ y_{WL} \\ z_{WL} \end{pmatrix} + \begin{pmatrix} x_{AL,i} \\ y_{AL,i} \\ 0 \end{pmatrix} \right] \otimes \mathbf{R}_{W_L A_{L,i}} \begin{pmatrix} D_{L,i} \\ 0 \\ L_{L,i} \end{pmatrix}\end{aligned} \quad (6)$$

Here $\mathbf{R}_{WB}$ is the rotation matrix between the wing frame and the body frame whereas (x_W, y_W, z_W) and ($x_{A,i}$, $y_{A,i}$, 0) correspond to the coordinates of the articulation wing point and the aerodynamic pressure center of the i^{th} wing element. Note that the indices R and L for lift and right wings respectively are deliberately removed in the following to simplify the expressions.

B. Aerodynamic forces

As shown on figure 1, the model of aerodynamic forces is based upon a local bi-dimensional approach: each wing is decomposed into a given number of parallel, chord-length elements, and the aerodynamic characteristics such as velocity $\mathbf{V}$ and angle of attack α are locally calculated for each element using aerodynamic 2D models.

For a given i^{th} wing element, the expression of the local aerodynamic velocity $\mathbf{V_i}$ is given by [17]:

$$\begin{aligned}\mathbf{V_i} &= -\mathbf{V_B} - \mathbf{\Omega_{EB}} \otimes \vec{BW} - \mathbf{\Omega_{EB}} \otimes \vec{WA}_i - \mathbf{\Omega_{BW}} \otimes \vec{WA}_i \\ &= -\mathbf{R}_{WE} \begin{pmatrix} u \\ v \\ w \end{pmatrix} - \mathbf{R}_{WB} \begin{pmatrix} p \\ q \\ r \end{pmatrix} \otimes \left[\mathbf{R}_{WB} \begin{pmatrix} x_W \\ y_W \\ z_W \end{pmatrix} + \begin{pmatrix} x_{A,i} \\ y_{A,i} \\ 0 \end{pmatrix} \right] \\ &- \mathbf{\Omega_{BW}} \otimes \begin{pmatrix} x_{A,i} \\ y_{A,i} \\ 0 \end{pmatrix}\end{aligned} \quad (7)$$

Where A_i is the aerodynamic centre of the i^{th} element and $\mathbf{\Omega_{BW}}$ the rotation vector between the wing and the body defined with the derivatives of the kinematic angles ξ, λ, μ, ν. More precisely, ξ is the angle of the stroke plane, λ the flapping angle, μ the deviation angle from the stroke plane and ν the pitch angle of the wing around its longitudinal axis. They correspond to the four possible rotations of the wing with respect to the body.

Then the local aerodynamic angle of attack α_i can be expressed as a function of the components of $\mathbf{V_i}$ within

$$\alpha_i = \angle\left(-V_{i,x} - \mathrm{j}V_{i,z}\right) \quad (\mathrm{j}^2 = -1) \quad (8)$$

Both components D_i, L_i of the aerodynamic forces can be represented within the aerodynamic frame of the i^{th} element as:

$$\begin{cases} L_i = L_i^{sta} + L_i^{rot} + L_i^{mass} \\ \quad = \frac{1}{2}\rho S_i \left|\mathbf{V_i}\right|^2 \left[C_{i,z}^{sta}(\alpha_i) + C_{i,z}^{rot}(\alpha_i) + C_{i,z}^{mas}(\alpha_i)\right] \\ D_i = D_i^{st} + D_i^{rot} + D_i^{mass} \\ \quad = \frac{1}{2}\rho S_i \left|\mathbf{V_i}\right|^2 \left[C_{i,x}^{sta}(\alpha_i) + C_{i,x}^{rot}(\alpha_i) + C_{i,x}^{mas}(\alpha_i)\right] \end{cases} \quad (9)$$

with the following aerodynamic coefficient functions respectively for the stationary, rotational, mass lift and drag:

$$\begin{cases} C_{i,x}^{sta} = k_{Cx_0} - k_{Cx_1}\cos(2\alpha_i) \\ C_{i,z}^{sta} = k_{Cz_1}\sin(2\alpha_i) \end{cases}$$

$$\begin{cases} C_{i,x}^{rot} = 2\pi\sin(\alpha_i)(3/4 + l_x/c)c\dot{\nu}/\left|\mathbf{V_i}\right| \\ C_{i,z}^{rot} = 2\pi\cos(\alpha_i)(3/4 + l_x/c)c\dot{\nu}/\left|\mathbf{V_i}\right| \end{cases} \quad (10)$$

$$\begin{cases} C_{i,x}^{mas} = (\pi/2)\sin(\alpha_i) y_{Ai} c\ddot{\lambda}/\left|\mathbf{V_i}\right|^2 \\ C_{z,x}^{mas} = (\pi/2)\cos(\alpha_i) y_{Ai} c\ddot{\lambda}/\left|\mathbf{V_i}\right|^2 \end{cases}$$

Where S_i, c, and l_x represent the surface, the chord and distance between the leading edge and the axis of rotation. k_{Cxo}, k_{Cx1}, k_{Cz1}, are constants based on measurements.

The elementary aerodynamic forces are then summed up and integrated within the earth frame, in order to obtain the translational and rotational velocities of the global MAV.

C. Bond Graph modeling

Figure 2 displays the bond graph schematic for the flapping wing MAV. In the actuation block, a mathematical description of the rotations angles of the wings are programmed (ξ, λ, μ, ν). It feeds the kinematics blocks for the right and left wings respectively. This block allows computing the rotation matrix, angular and translational velocities. For example, the rotation matrix $\mathbf{R}_{WB}$ between the wing frame and the body frame, as well as the rotation matrix $\mathbf{R}_{EW}$ between the earth frame and the wing frame which are inputs of the aerodynamic velocity block. Then the velocity block solves equation 7 whereas the aerodynamic forces block computes equation 5, 6 and 8-10.

Note that only the left side of the model is depicted in figure 2 as it is a symmetric model. Aerodynamic forces and velocities are also side dependant, whereas the dynamic block where the Newton-Euler equations are solved is common to both wings as all moments and forces (right and left) are taken into account.

Then the Bond graph representation of the Newton Euler equations (1)-(2) is shown in Figure 3 where the upper triangle relates the energy flow in translational dynamics and the lower triangle defines rotational dynamics. The three 1-junctions both in the upper and lower triangles provide the nodes for external forces and moments respectively.

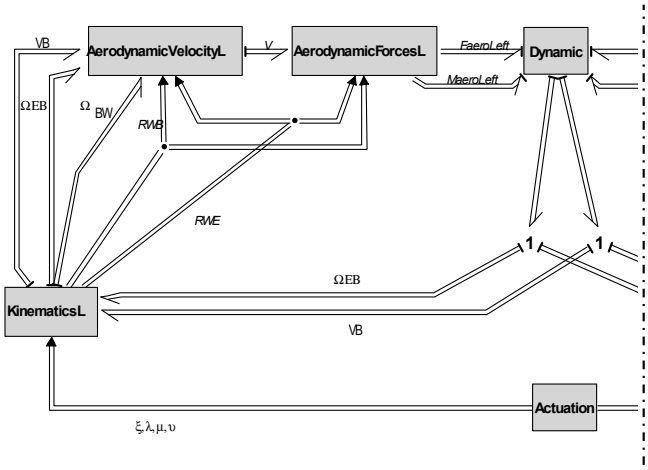

Fig. 2. Bond graph schematic of the flapping wing MAV (left side).

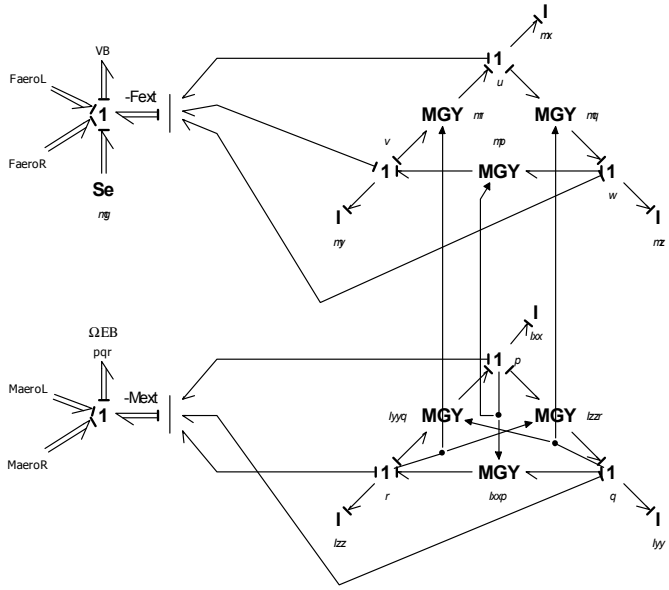

Fig. 3. Bong graph representation of Newton-Euler equations.

III. Results and Discussion

To validate the bond graph model, open loop simulations have been performed. It is worth mentioning that the open loop system is unstable, as a consequence, in the model development, we have introduced the possibility to lock each of the 6 degrees of freedom of the system (3 in translation, 3 in rotation). The first step is to lock all of them as in this static configuration; a comparison with experimental results on flapping wing robots is possible [14]. Then, the study of motion along one axe is possible, such as elevation / descent when the z_E translational degree of freedom is unlocked.

A. Validation of the aerodynamic model

Aerodynamic velocities and aerodynamic efforts have been calculated and compared to measurements available in the literature.

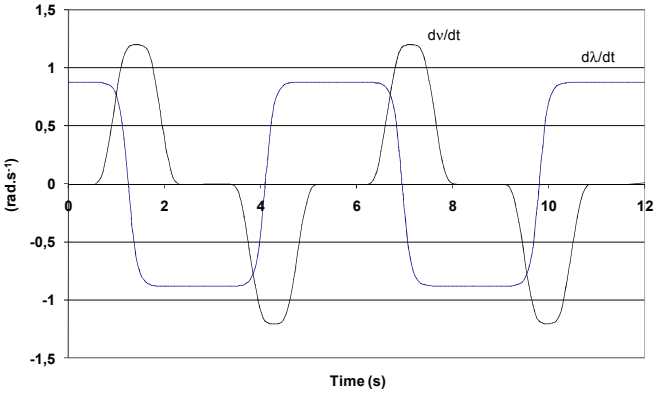

Fig. 4. Flapping and pitch angular velocities.

A mathematical description of flapping wing insects was programmed to mimic wing kinematics, namely: flapping and pitch angle. In the case of wings insects $\mu = 0$, moreover, the case considered here for validation, a flapping robot, requires to take $\xi = 0$. A typical evolution of the derivatives: $d\lambda/dt$ and dv/dt is displayed Figure 4. The periodic laws define the input signals for our simulations; the pitch angle is a square like function as it has been shown that incidence is quite constant during stroke. They have been parameterised in order to be able to compare our simulations with the Robotfly experimental results [14].

Figures 5 and 6 represent the evolution of the local aerodynamic horizontal (V_{xi}) and vertical (V_{zi}) velocities as a function of time, each curve being the result obtained for one of the 10 slices the wing has been devised into (i=1 represents the slice of the wing the closer to the wing hinge point). It is observed that aerodynamic speeds are increasing as a function of distance along the wing as expected. This results in the evolution of the aerodynamic velocity norm, figure 7.

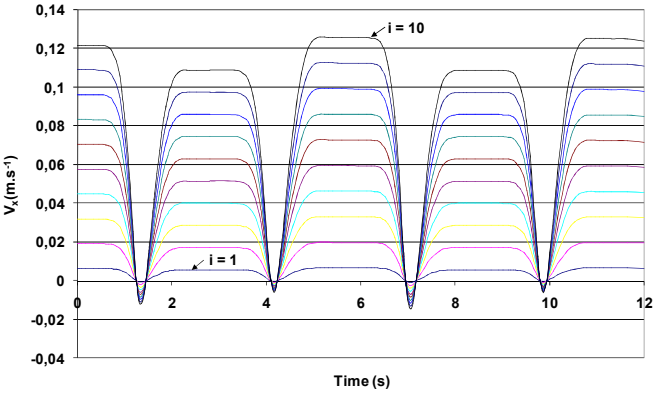

Fig. 5. Local aerodynamic horizontal velocity (V_{xi})

The evolution of lift forces are depicted by figure 8, it represents the steady lift force and the rotational lift forces. Both forces depend on the local aerodynamic norm. Moreover, it can be observed that the rotational lift force evolution depends also on the pitch angle derivative. In figure 9 evolution of the total lift force is plotted. Both qualitative

evolution and quantitative value of experimental results are well reproduced [14].

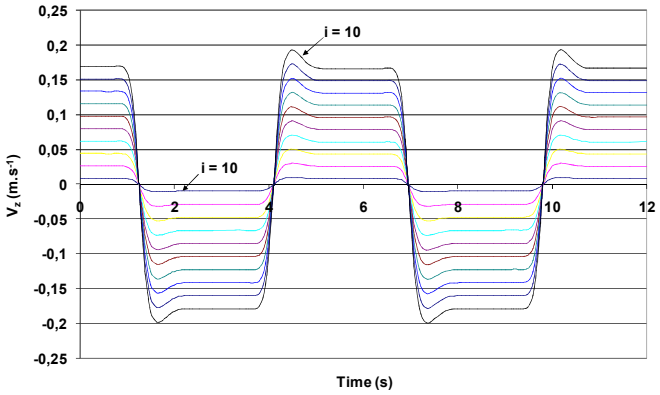

Fig. 6. Local aerodynamical horizontal velocity (V_{zi})

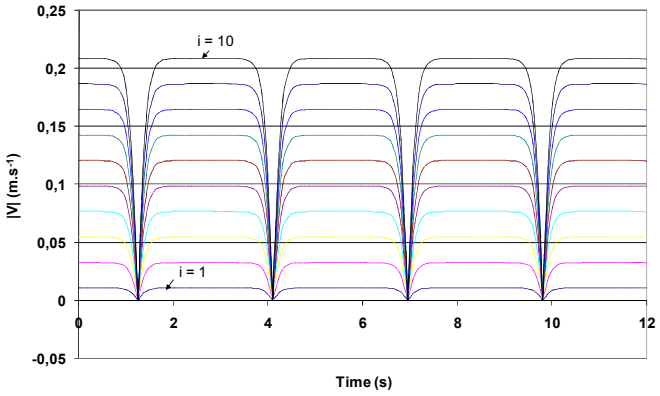

Fig. 7. Local aerodynamic velocity norm

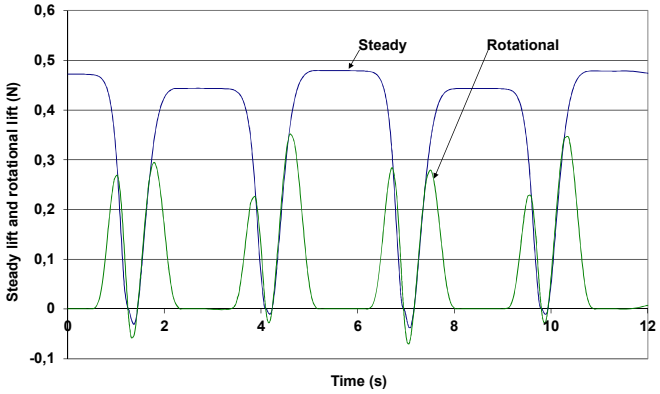

Fig. 8. Rotational and steady lift forces

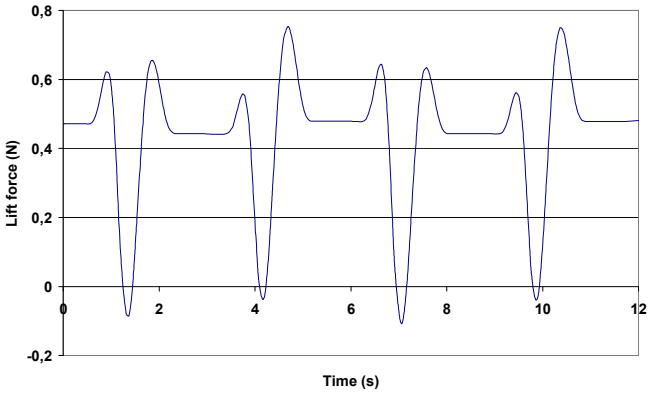

Fig. 9. Total Lift Force

B. *Dynamic model*

One degree of freedom has then been released: translation along z_E-axis. This allows us to study the displacement, position, velocity, along this axis. In particular we want to verify the influence of the forces produced by the flapping of the wing on the MAV motion.

Figure 10 displays the evolution of the velocity w along z_E - axis, it corresponds to a free fall of the MAV: only the weight is taken into account. Figure 11 illustrates that, when the flapping frequency is no more null, the total lift force produces a force that is sufficient to slow down the falling of the MAV.

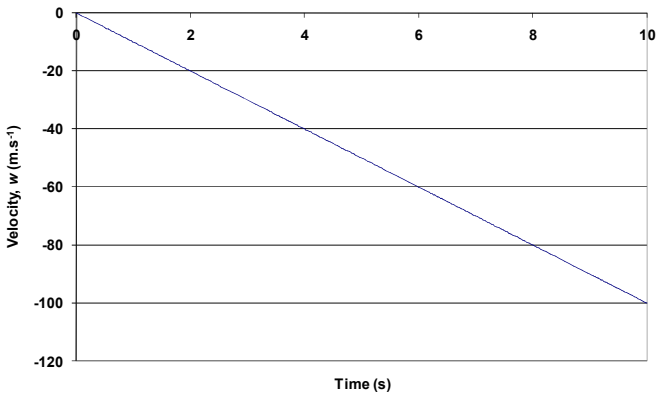

Fig. 10. Evolution of the ascention velocity, open Loop Free Fall Simulation for zero thrust.

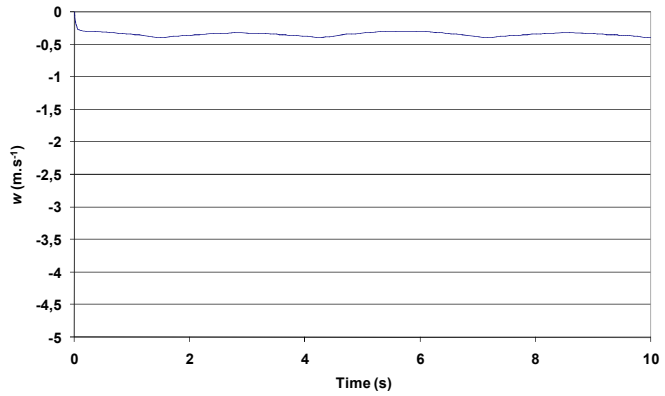

Fig. 11. Evolution of the ascention velocity, open Loop Free Fall Simulation with sinusoïdal flapping.

IV. Conclusion

In this paper we have introduced bond graph modelling to the field of flapping wing MAV aerodynamics. This model has been validated thanks to experimental published results. Bond graph modelling enables an efficient approach of complex and coupled dynamics modelling, as illustrated by this paper. Flapping wing MAV is a mechatronic system, as such, the concern about different energies domains is crucial: in our approach, next step is to merge this model with the model of power transmission of a flapping wing nano air vehicle [16].

It is well know that the bond graph approach also facilitates extension of the model to include control concerns, future extensions of the model will be connected with regulation laws. Moreover, thanks to the discrete nature of the wing model, this model can be improved by taking into account in a future development the flexibility of a real wing.

References

[1] http://www.imav2013.org/index.php/conference-proceedings.html

[2] H. Tanaka, K. Hoshino, K. Matsumoto, and I. Shimoyama, "Flight dynamics of a butterfly-type ornithopter," IEEE/RSJ Int. Conf. on Intelligent Robots and Systems, Edmonton, Alberta, Canada, 2005.

[3] C.T. Bolsman, J.F.L. Goosen, and F. van Keulen, "Design Overview of a Resonant Wing Actuation Mechanism for Application in Flapping Wing MAVs," International Journal of Micro Air Vehicles, Vol. 1, No. 4, pp. 263-272, 2009.

[4] Keennon M., Klingebiel K., Won H., Andriukov A., "Developpment of the nano hummingbird : a tailless flapping wing micro air vehicle," 50th AIAA Aerospace sciences meeting -2012- Nashville.

[5] D.J. Pines and DARPA/DSO, Nano Air Vehicle Program, *BAA06-06.*

[6] R. Wood, S. Avadhanula, R. Sahai, E. Steltz and R. Fearing, "Microrobot Design Using Fiber Reinforced Composites," J. Mech. Des., Vol. 130, 052304 (11 pages), 2008.

[7] X.Q. Bao, A. Bontemps, S. Grondel, E. Cattan, "Design and fabrication of insect-inspired composite wings for MAV application using MEMS technology," J. Micromech. Microeng., Vol. 21, 125020-1-16, 2011.

[8] A. Bontemps, T. Vanneste, J. B. Paquet, T. Dietsch, S. Grondel, E. Cattan, "Design and performance of an insect-inspired nano air vehicle," Smart Mater. Struct., Vol. 22, 13 p., 2013.

[9] B. Etkin, and L. Reid, Dynamics of Flight, Wiley, New York, 1996.

[10] D. Doman, M. Oppenheimer, and D. Sigthorsson, "Dynamics and control of a minimally actuated biomimetic vehicle: Part i - aerodynamic model," Proceedings of the AIAA Guidance, Navigation, and Control Conference, Chicago, Illinois, USA, August 10-13, 2009. AIAA, 2009.

[11] M. Oppenheimer, D. Doman, and D. Sigthorsson, " Dynamics and control of a minimally actuated biomimetic vehicle: Part ii – control," Proceedings of the AIAA Guidance, Navigation, and Control Conference, Chicago, Illinois, USA, August 10-13, 2009. AIAA, 2009

[12] R.J. Wood, "The first takeoff_of a biologically inspired at-scale robotic insect," IEEE Transactions on Robotics, Vol. 24, pp.341-347, 2007.

[13] T. Hedrick, and T. Daniel, "Flight Control in the Hawkmoth Manduca Sexta: The Inverse Problem of Hovering," Journal of Experimental Biology, Vol. 209, No. 16, pp. 3114–3130, 2006.

[14] Dickinson, M. H., Lehmann, F. O., & Sane, S. P., "Wing rotation and the aerodynamic basis of insect flight", Science, 284(5422), 1954-1960, 1999.

[15] N. O Perez-Arancibia, K.Y. Ma, K. C. Galloway, J. D. Greenberg and R. J. Wood, "First controlled vertical flight of a biologically inspired microrobot," Bioinsp. Biomim., Vol. 6, 036009, (11pp), 2011.

[16] A. Bontemps, S. Grondel, T. Vanneste, S. Dupont, E. Cattan, "Modeling and evaluation of power transmission of flapping wing nano air vehicle," submitted to 10th IEEE/ASME International Conference on Mechatronics Systems and Applications, 2014.

[17] T. Rakotomamonjy, T. Le Moing, B. Danet, X. Gadoullet, D. Osmont, M. Dupont, "Evaluation of flexoble flapping concept," Proc. of SPIE , Vol. 7295, 72951J, 2009.